Journal of Hazardous Materials 177 (2010) 762–772

Contents lists available at ScienceDirect

Journal of Hazardous Materials

journal homepage: www.elsevier.com/locate/jhazmat

Neutralization of acid mine drainage using the final product from CO_2 emissions capture with alkaline paper mill waste

Rafael Pérez-López [a,b,*], Julio Castillo [b], Dino Quispe [b], José Miguel Nieto [b]

[a] Institute of Environmental Assessment and Water Research, IDÆA – CSIC, Jordi Girona 18, 08034 Barcelona, Spain
[b] Department of Geology, University of Huelva, Campus 'El Carmen', 21071, Huelva, Spain

ARTICLE INFO

Article history:
Received 3 November 2009
Received in revised form
21 December 2009
Accepted 22 December 2009
Available online 4 January 2010

Keywords:
Paper waste
CO_2 sequestration
Acid mine drainage
Neutralization
Trace elements

ABSTRACT

In this study, experiments were conducted to investigate the applicability of low-cost alkaline paper mill wastes as acidity neutralizing agents for treatment of acid mine drainage (AMD). Paper wastes include a calcium mud by-product from kraft pulping, and a calcite powder from a previous study focused on sequestering CO_2 by carbonation of calcium mud. The neutralization process consisted of increase of pH by alkaline additive dissolution, decrease of metals solubility and precipitation of gypsum and poorly crystallized Fe–Al oxy-hydroxides/oxy-hydroxysulphates, which acted as a sink for trace elements to that extent that solutions reached the pre-potability requirements of water for human consumption. This improvement was supported by geochemical modelling of solutions using PHREEQC software, and observations by scanning electron microscope and X-ray diffraction of reaction products. According to PHREEQC simulations, the annual amount of alkaline additive is able to treat AMD (pH 3.63, sulphate 3800 mg L^{-1}, iron 348 mg L^{-1}) with an average discharge of about 114 and 40 L s^{-1} for calcium mud and calcite powder, respectively. Likewise, given the high potential of calcium mud to sequester CO_2 and of resulting calcite powder to neutralize AMD, paper wastes could be a promising solution for facing this double environmental problem.

1. Introduction

Acid mine drainage (AMD) is an inevitable wastewater of the mining industry characterized by its strongly acidic nature and significant levels of metal ions, especially iron, and sulphate. AMD results from the percolation of water through sulphide minerals from waste disposal sites in sulphide-mining districts, generally pyrite, which oxidizes and dissolves when in contact with air and water. These discharges are typically the first cause of environmental deterioration of fluvial courses, groundwater and soils. Treatment of AMD can take two basic ways: active and passive techniques [1]; albeit, passive technologies have received much more attention recently since the improvement of water quality occurs using only naturally available energy sources and, once built, require sporadic maintenance [2]. The most common passive systems to treat AMD are anoxic limestone drains (ALD; [3]), reducing and alkalinity producing systems (RAPS; [4]) and the dispersed alkaline substrate (DAS; [5]).

Most of AMD treatment systems use limestone as an acidity neutralizing agent in order to increase pH and enhance metal precipitation (e.g. [6]). However, the use of limestone implies a high economic and environmental cost because limestone is usually a "resource" and not a "residue". The objective of integrated waste management is the search for sustainable development, i.e. to balance the fulfilment of human needs with the protection of the natural environment in the present and indefinite future. With this in mind, the current work is focused on recycling a waste as an alkaline additive in passive treatment systems in a geological setting that represents a clear example of an AMD-affected region, in addition to suffering other huge environmental problems. Ideally, the perfect additive for the AMD treatment must fulfil the following requirements: high acid neutralizing potential, low-cost and production close to the environmental problem.

2. Objectives and environmental setting

This research was carried out in the Province of Huelva (SW, Spain), which is characterized from an environmental point of view by two continuous pollution sources: abandoned mining activity from the Iberian Pyrite Belt (IPB) and the present industrial activity from the Huelva Industrial State. IPB, located at approx. 50 km from the city of Huelva, is one of the most important metallogenetic provinces of polymetallic massive sulphides in the world [7]. The zone waked up the economic and commercial interest of numerous civilizations from immemorial times [8]. The result of the intense

* Corresponding author at: Department of Geology, University of Huelva, Campus 'El Carmen', 21071 Huelva, Spain. Tel.: +34 95 921 9826; fax: +34 95 921 9810.
E-mail address: rafael.perez@dgeo.uhu.es (R. Pérez-López).

0304-3894/$ – see front matter © 2009 Elsevier B.V. All rights reserved.
doi:10.1016/j.jhazmat.2009.12.097

mining exploitation is a region totally degraded in which original orography has been replaced by enormous open pit mines and numerous piles of mining wastes (approx. 2×10^8 m^3). However, the environmental impact of main relevance derives from AMD production as a result of the oxidation of sulphides contained in these residues. These acidic discharges are drained by the fluvial courses (Tinto and Odiel rivers) which transport a huge amount of metals to a common estuary, so-called "Ría de Huelva" Estuary, and later to the Atlantic Ocean. Olías et al. [9] estimated that the media discharge of contaminants achieving the ocean is 7900 t year^{-1} of Fe, 5800 t year^{-1} of Al, 3500 t year^{-1} of Zn, 1700 t year^{-1} of Cu and 1600 t year^{-1} of Mn, in addition to minor amounts of other metals (Co, As, Ni, Pb, Cd).

On the other hand, the relatively flat surface of the estuarine system, the nearby water availability and the proximity of the sea as a communication via have made that this area, like other estuarine areas in Europe, has undergone an extensive industrialization process since the 1960s with the development of a huge chemical–metallurgical complex of industries located at 1–2 km from the city of Huelva [10]. One of the main industrial activities is focused on the production of pulp for paper manufacture in a local kraft mill (ENCE Company). The dominant process for cellulose pulp production involves cooking woodchips in high concentrations of sodium hydroxide and sodium sulphide for 2–4 h at 170 °C. This process, known as kraft pulping, favours the lignin dissolution and the separation of the cellulose fibers that are recovered by means of sieving. The residual liquids or black liquor containing the most of the dissolved lignin are transformed to white liquor and reused in the cooking stage. This transformation is carried out by both combustion in a boiler and causticizing with lime and implies the production of several types of calcium-rich solid wastes with alkaline nature known generically as alkaline paper mill wastes.

In some pulp and paper industries, the alkaline by-products are usually sold for the cement manufacture and as alkaline amendment for agricultural soils. Nevertheless, their recycling is limited by the presence of chloride and metals, and in numerous occasions must be stored near the industrial facilities. Few investigations focused on searching possible applications to alkaline paper mill wastes have been reported in the literature, and the existing ones are based on their application in separate for the neutralization of acid mine drainages [11] and for the reduction of carbon dioxide greenhouse gas emissions into the atmosphere using CO_2 mineral sequestration [12]. The main aim of this paper is to utilize the alkaline wastes from cellulose pull production in Huelva in order to treat jointly a double environment problem in the zone, on the one hand, the emission of residual CO_2 gaseous produced by the cellulose plant and, on the other hand, the production of AMD-discharges generated from sulphide oxidation in abandoned mining districts of the IPB. To this end, both alkaline wastes obtained directly from ENCE in Huelva and solid products resulting from the sequestration process of CO_2 obtained in previous studies [12] are evaluated as acidity neutralizing agents for passive treatment of AMD by means of a series of laboratory experiments. From the sustainable development point of view, the approach proposed is especially attractive since a low-cost residue is used to face several environmental issues, and moreover within the same area, which would further cheapen the transporting costs in future remediation plans.

3. Materials and methods

3.1. Sample description

3.1.1. Acid mine waters

Two yellow-reddish drainages emanating from IPB sulphide-rich wastes were used as natural reagent solutions for neutralization experiments: (1) from Cueva de la Mora mining district (AMD_{CM}), whose hydrogeochemical facies of AMD conforms to average of typical mine waters from the IPB, and (2) from Tharsis mining district (AMD_{TH}), which is characterized by higher both acidity and pollutant concentration than the remaining drainages [13]. Of each discharge, a water sample (ca. 2 L) was taken with a polyethylene bottle and filtered through a 0.45-μm Teflon filter within 24 h of its collection for chemical analysis and experiments.

3.1.2. Alkaline additives

The alkaline paper wastes were kindly ceded by pulp mill ENCE in Huelva. The by-product used in this study, so-called calcium mud, is the waste of the calcination or conversion of calcium carbonate to lime for the causticizing of the black liquor. Calcium mud was selected since it presents a higher Ca content than the remaining alkaline paper wastes. A representative sample (approx. 2 kg) was collected in the factory as a staring material using a polypropylene shovel, and transferred to clean polypropylene bags. In the laboratory, sample was oven-dried (40 °C) until complete dryness, grounded in an agate mill to less than 63 μm, homogenized and divided into two portions: one for the CO_2 sequestration experiments and another for the AMD neutralization experiments.

The presence of high concentrations of portlandite ($Ca(OH)_2$) in calcium mud (see Section 4.1) accounts for the high alkalinity and potential for CO_2 sequestration by aqueous carbonation as discussed below, although full details can be found elsewhere [12]. In that work, the CO_2 sequestration experiments were conducted in a 2 L closed titanium-lined pressure reactor (Parr Instrument Co., USA, Model 4843) charged with Millipore MQ water (18.2 MΩ) and paper mill waste. The CO_2 gas was injected into the reactor by opening a valve and adjusting the pressure to the desired one. In this aqueous system, the water–CO_2-paper waste interaction supposed the Ca release from the portlandite dissolution, CO_2 dissolution in water and calcite ($CaCO_3$) precipitation. The overall reaction for the process can be written as (Eq. (1)):

$$Ca(OH)_2(s) + CO_2(aq) \rightarrow CaCO_3(s) + H_2O \quad (1)$$

Thus, the gas CO_2 was transformed and sequestered to stable carbonate minerals. During aqueous carbonation process, the main trace metals initially contained in the alkaline waste were released in solution and captured by calcite precipitation. The result was a free-metal solution in contact with a calcite-rich solid named as calcite powder. Although in a trace proportion, this sub-product could contain pollutant elements that reduce drastically its applicability. Albeit, a very advantageous and viable possibility would be to use calcite as alkaline additive in acidic waters already contaminated by metals and with a scarcity of nutrients and organic matter. In fact, this possibility aims to be demonstrated in the current paper.

3.2. Neutralization reactions

The neutralization experiments were conducted through the interaction of alkaline additive and AMD in centrifuge tubes under continuous stirring on an orbital shaker rotating at room temperature and 12 rpm, thus allowing full contact between the solid particles and the aqueous solution for different lengths of time. The AMD was stirred for 30 min for equilibration before the alkaline additive was added. Four series of interactions were carried out using solid:liquid ratios of 1:400 and 1:80 for experiments with AMD_{CM} and AMD_{TH}, respectively. Hereafter (even in figure and table captions), AMD_{CM}-CM refers to interaction between 40 mL of AMD_{CM} and 0.1 g of calcium mud, AMD_{CM}-CP to interaction between 40 mL of AMD_{CM} and 0.1 g of calcite powder, AMD_{TH}-CM to interaction between 40 mL of AMD_{TH} and 0.5 g of calcium mud and AMD_{TH}-CP to interaction between 40 mL of AMD_{TH} and 0.5 g of calcite powder. Each series of experiments is composed of 12

sub-samples in which reaction is stopped at designated time intervals: approx. 0 min, 5 min, 15 min, 40 min, 2 h, 6 h, 12 h, 24 h, 48 h, 96 h, 216 h and 290 h. At the end of each sub-sample, the centrifuge tube was removed from the shaker and the supernatant was separated from the solid product by centrifugation at 4000 rpm for 3 min. Finally, the supernatant solutions were filtered through a 0.45-μm Teflon filter and the solid product was dried directly in the centrifugation flasks at 40 °C.

3.3. Analytical techniques

Total element concentration of the calcium mud was analyzed by Acme Analytical Laboratories Ltd. (Vancouver, Canada), accredited under ISO 9002, through its Italian affiliate (ERS Srl, Napoli). The analysis was determined by inductively coupled plasma-atomic emission spectroscopy (ICP-AES; Jarrel Ash Atomcomp 975) and inductively coupled plasma-mass spectroscopy (ICP-MS; PerkinElmer Elan 6000) following an aqua regia digestion ($1HCl{:}1HNO_3{:}1H_2O$) at 90 °C for 1 h that dissolves fully carbonate minerals. Precision of the analysis was calculated using three in-house replicates. Accuracy was estimated from analysis of Acme's in-house reference materials, DS7 and SO-18. Reference materials DS7 and SO-18 were calibrated to an aqua regia digestion against published values for a concentrated HCl and HNO_3 digestion of the Canadian Certified Reference Materials Project (CCRMP) TILL-4 and LKSD-2.

The acid mine waters and supernatant solutions obtained in the experiments were collected and before being filtered pH, electrical conductivity (EC) and redox potential (Eh) were measured immediately to avoid producing dissolution effects of CO_2 (g) and O_2 (g) on the pH and Eh of the solutions. Both pH and EC were measured using Crison instruments and Eh was measured using a Hanna measurer with Pt and Ag/AgCl electrodes (Crison). Eh measurements were corrected to standard hydrogen electrode. Later, the samples were filtered, acidified to pH < 2 with HNO_3 (2%) suprapur and stored at 4 °C in polyethylene bottles until analysis. The concentration of a suite of elements that commonly occur in AMD systems was analyzed at the Central Research Services at Huelva University by means of ICP-AES on a Jobin Yvon (JY ULTIMA 2) spectrometer, using a specific method for the analysis of major and trace elements that was contrasted with international and natural calibrated standards [14].

The mineralogical characterization of alkaline additives and final reaction products was carried out by X-ray diffraction (XRD, powder method) using a Bruker diffractometer (model D8 Advanced). Working conditions were slit fixed at 12 mm, Cu Kα monochromatic radiation, 20 mA and 40 kV. Samples were run at a speed of 2° 2θ/min (3–65°). Fluorite as internal reference material was used to determine semi-quantitative mineralogical composition. In order to complete the mineralogical characterization, samples were also observed by means of a scanning electron microscopy (SEM; JEOL JSM-5410) equipped with an energy dispersive system (EDS; Link-Oxford) for the chemical microanalysis.

3.4. Thermodynamic approach

Precipitation of newly formed solid phases could chemically control the fate of AMD contaminants in the neutralization reactions. This process may be predicted from supernatant solutions by a thermodynamic model and must be corroborated by characterization of final solid products. Equilibrium geochemical speciation/mass transfer model PHREEQC [15] with the database of the speciation model MINTEQ [16] was applied to determine aqueous speciation of leachates and saturation indices of solid phases [$SI = \log(IAP/K_S)$, where SI is the saturation index, IAP is the ion activity product and K_S is the solid solubility product]. Zero, negative or positive SI values indicate that the solutions are saturated, undersaturated and supersaturated, respectively, with respect to a solid phase. For a state of subsaturation, dissolution of the solid phase is expected and supersaturation suggests precipitation.

Table 1
Compilation of pH, electrical conductivity and chemical composition of the starting materials of the neutralization experiments.

	Starting materials		
	AMD_{CM}	AMD_{TH}	Calcium mud
pH	3.63	2.24	11.96
EC ($mS\,cm^{-1}$)	4.63	8.01	–
Major elements (%)			
Al	0.01	0.04	0.03
C	na [a]	na	3.0 [b]
Ca	0.03	0.02	59
Fe	0.03	0.15	0.05
K	0.0002	0.0004	0.07
Mg	0.03	0.10	0.18
Na	na	na	1.2
P	na	na	1.2
S	0.13	0.41	1.0
Trace elements (ppm)			
As	0.45	4.5	3.2
Cd	0.43	0.38	0.25
Cu	2.2	46	25
Cr	3.7 [c]	0.15	24
Ni	0.81	1.8	13
Zn	399	322	36

[a] na: not analyzed.
[b] Determined by LECO total carbon analyzer.
[c] Concentration in ppb.

4. Results and discussion

4.1. Characterization of the starting materials

Results of chemical characterization of the starting materials are reported in Table 1. Both mine water samples are strongly acidic, with pH values of 2.24 and 3.63 for AMD_{TH} and AMD_{CM}, respectively. These low pH values imply a lack of calcareous minerals and absence carbonate buffering within mine tailings in both mining districts, although this is a common feature in the entire IPB [13]. Higher polluting levels are usually found in the acid leachates from the huge waste piles of Tharsis mining district, which indicate a very intense oxidation and subsequent dissolution of pyrite and the accompanying sulphides (chalcopyrite, sphalerite, galena, arsenopyrite). In fact, the sampled AMD_{TH} is one of the discharges that most profusely contribute to contamination in the Odiel river, through Meca stream [17]. Its pH value matches an extremely high EC ($8.01\,mS\,cm^{-1}$), sulphate concentration ($12{,}400\,mg\,L^{-1}$) and other potentially toxic metals (Table 1). The waters of the Cueva de la Mora mining district have also high EC value ($4.63\,mS\,cm^{-1}$), sulphate ($3800\,mg\,L^{-1}$) and metal concentration (Table 1), although not as extreme in comparison with Tharsis but rather comparable to average facie of IPB mining districts.

The extreme acidity of both AMD is in contrast to alkaline nature of the solid additives. When calcium mud and calcite powder were added to distilled water in a solid/liquid ratio of 1:2.5, the pH of the suspension increased to 11.96 and 10.01, respectively, in a few minutes, thereby reflecting their strong neutralizing potentials. Calcium mud is made up of portlandite ($Ca(OH)_2$; 55 wt%), calcite ($CaCO_3$; 33 wt%) and hydroxyapatite ($Ca_{10}(PO_4)_6(OH)_2$; 12 wt%). The portlandite particles present a laminar-pseudohexagonal habit, as observed by SEM (Fig. 1a). The chemical composition shows mainly high content of Ca (59 wt%), C (3.0 wt%) and appreciable amounts of P, Na, S, Mg, K, in this order of abundance, as well as a

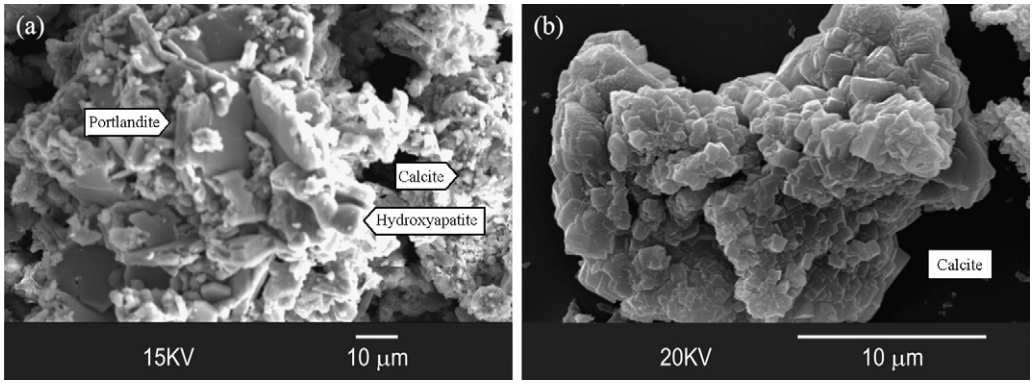

Fig. 1. SEM images of (a) calcium mud showing the initial crystals of portlandite, calcite and hydroxyapatite and (b) calcite powder precipitated during CO_2 sequestration experiments. Images were previously published in Pérez-López et al. [12].

variety of trace elements in concentrations even higher than acid mine waters (Table 1), reason that causes the drastic reduction of applicability of these wastes. After CO_2 sequestration process using calcium mud, and according to Eq. (1), the portlandite (55 wt%) is totally carbonated and transformed to calcite. Hydroxyapatite seems not to be involved in the CO_2 sequestration process. As a consequence, calcite powder is composed of calcite (88 wt%) and hydroxyapatite (12 wt%). Metal concentrations in the final calcite imply a high transfer factor of around 100 and 75% for main toxic metals [12,18]. The newly formed calcite is characterized by micrometric agglomerates of rhombohedral-crystals (Fig. 1b).

4.2. Effect of interactions on solutions chemistry

The variations in pH, EC and sulphate concentration as a function of time in the solutions resulting from four interactions are shown in Fig. 2. In all experiments, reaction achieved steady state conditions at approx. 48 h, which was verified by a series of constant values that differed less than 5%. Interaction of AMDs with alkaline additives resulted in the effective acidity neutralization and a significant decrease in conductivity, and therefore, in the pollutant load. The initial pH of both AMDs increased until values ranging 7.8–8.3 and 6.1–7.1, whereas EC decreased until values of approx. 2.2 and 3.6 mS cm^{-1} at the steady state, for the interactions with calcium mud and calcite powder, respectively. The decrease of EC values reflects a possible improvement in the quality of AMDs that was confirmed by the decrease of sulphate concentration in solution. In fact, sulphate concentration at the steady state dropped in AMD_{TH} until 2600 and 5000 mg L^{-1} and in AMD_{CM} until 2500 and 3200 mg L^{-1} by interaction with calcium mud and calcite powder, respectively (Fig. 2c). On the other hand, the behaviour of Fe in solution is very significant: with the exception of the first leachates, the rest of them contain Fe concentrations below the detection limit for all interactions.

The concentrations of Al, As, Cu and Cr are also characterized because with time are very close, and even lower in most cases, to the detection limit of ICP-AES. However, the concentrations of Zn, Ni and Cd are totally depleted in solution only in the experiments with calcium mud, whereas these metals are retained partially in experiments with calcite powder. In these last experiments, the lowest concentrations were of 169 and 73 mg L^{-1} for Zn, 0.46 and 1.42 mg L^{-1} for Ni, and 90 and 50 μg L^{-1} for Cd, in the interactions with AMD_{CM} and AMD_{TH}, respectively.

The improvement in the quality of resulting solutions has been so effective that the final concentrations of Fe, Al, Cu, As, Cr, Zn, Ni and Cd in four interactions were adjusted to the pre-potability requirements of water for human consumption according to European legislation (Directive 98/83/CE, DOCE L No. 330 on 5th

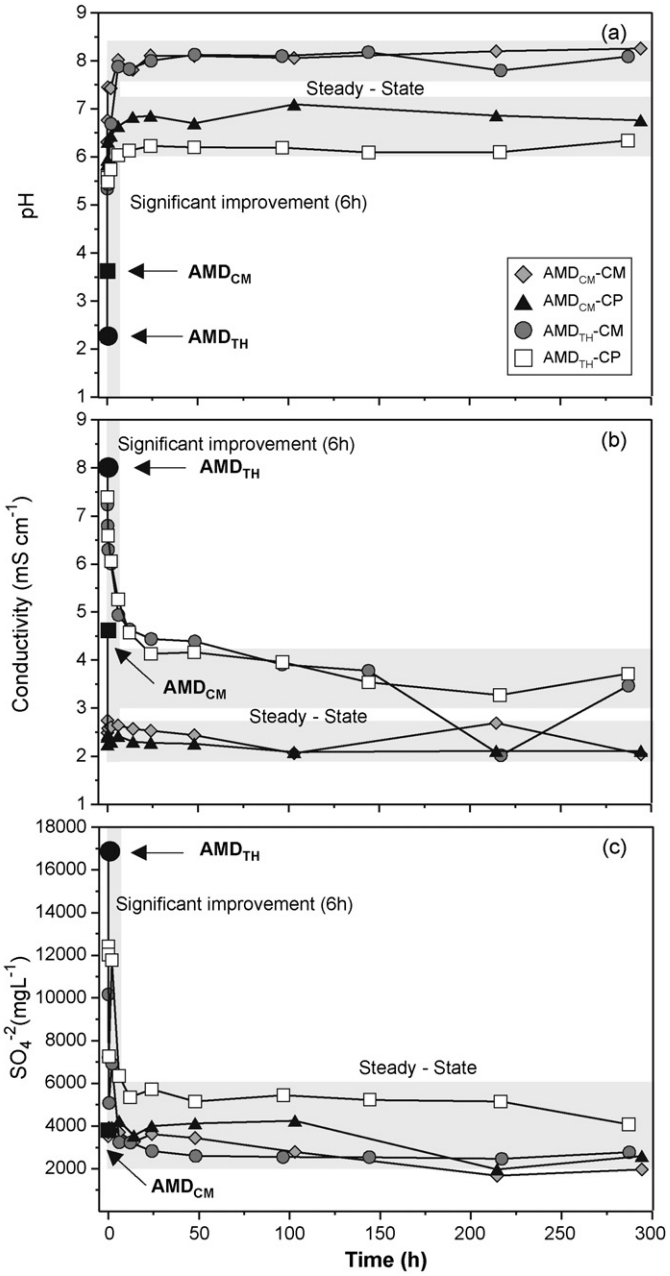

Fig. 2. Variation in (a) pH, (b) conductivity and (c) sulphate concentration as a function of time in the leachates from the neutralization experiments.

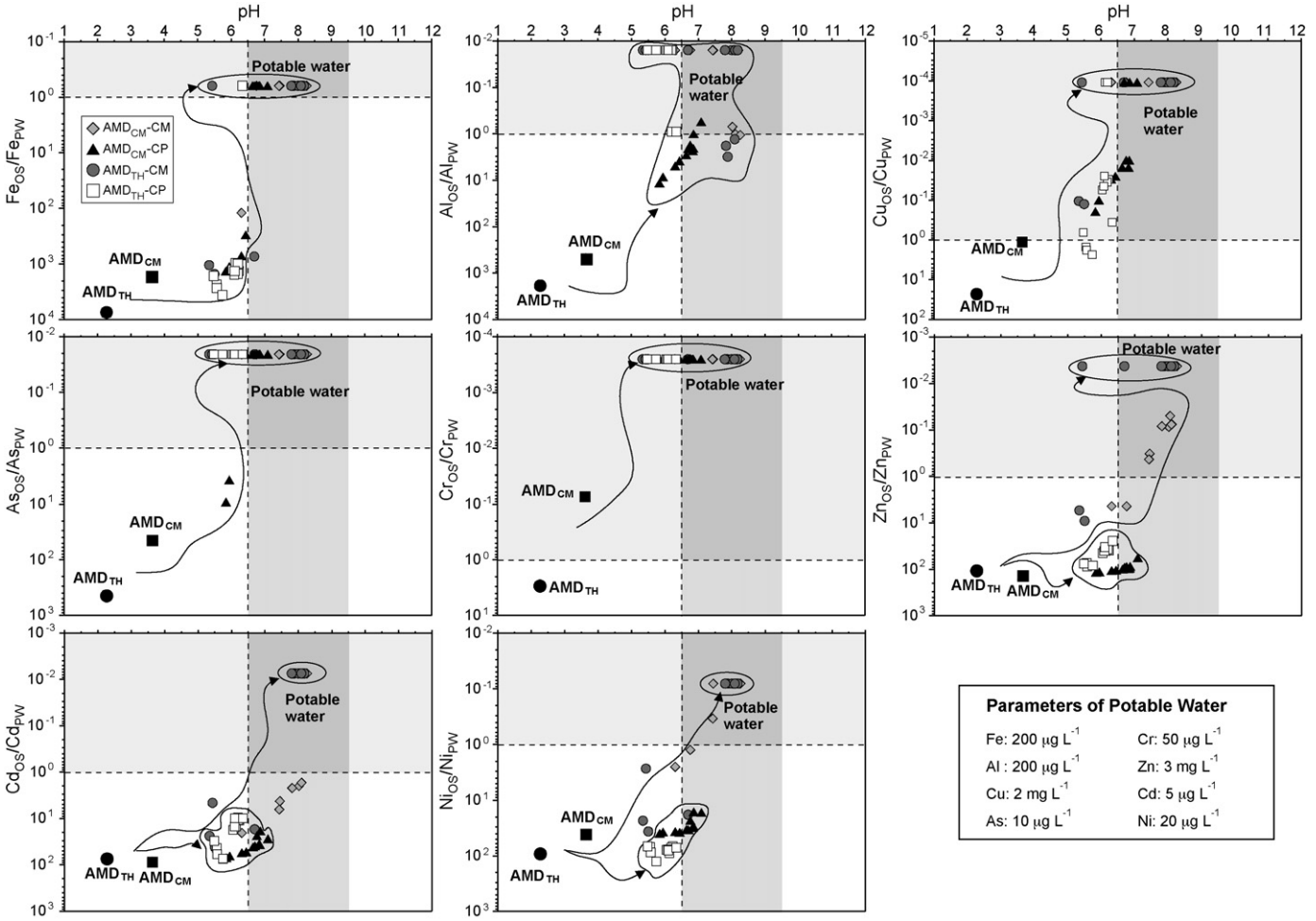

Fig. 3. Variation in the output concentrations of iron, aluminium, copper, arsenic, chromium, zinc, cadmium and nickel as a function of pH in the leachates from the neutralization experiments. Values of output solutions (OS) were normalized with respect to parameters of potable water (PW).

December 1998), with exception of Zn, Cd and Ni concentrations in the experiments with calcite powder (see Fig. 3). This improvement occurs even despite the significant additional amounts of toxic elements contained in both alkaline additives and that are released into solution during the neutralization experiments.

4.3. Characterization of the final solid products

Comparison of X-ray diffraction spectra of the starting material and the final solid products obtained from neutralization experiments demonstrates that (Fig. 4): (1) the portlandite contained in the calcium mud is totally dissolved when interacting with both AMDs; (2) unlike the calcite and hydroxyapatite contained in the calcium mud and calcite powder, that are not entirely consumed during the neutralization reaction but a small unreacted proportion remains at the end of all experiments; and (3) gypsum is the only crystalline phase newly formed during the four long-term interactions. If precipitation of other newly formed phases occurs during neutralization experiments it is assumed, therefore, that correspond to amorphous or poorly crystalline phases, as they do not diffract X-rays.

Results obtained from the morphological analysis of the final solid products using SEM-EDS are similar in all interactions. SEM observations confirmed the appearance of newly formed gypsum crystals that occur as well-developed euhedral monoclinic laths with tabular habit of up to 100 μm long (Fig. 5a). Visual observations of reacted samples after experiments indicated the occurrence of Fe-rich secondary phases owning to the rust-coloured stains. A more exhaustive examination with SEM-EDS confirmed that Fe was present as botryoidal microaggregates of phases chemically composed also by S, Al and minor Ca, Zn Cu and Mn (Fig. 5b). Non-detection of these Fe-phases in the solid residues by XRD must probably be due to their amorphous nature.

4.4. Mechanisms of metal removal in solution

The thermodynamic modelling of the solutions resulting from the neutralization process should explain what is observed in the mineralogical characterization of the final solid products. This agreement would facilitate finding out mechanisms involved in the retention processes of metals in solution. The acidity neutralization is a consequence of both portlandite and/or calcite dissolution when interacting with the AMD-sulphuric acid (Eqs. (2) and (3)):

$$Ca(OH)_2(aq) + H_2SO_4 \rightarrow Ca^{2+} + SO_4^{2-} + 2H_2O \quad (2)$$

$$CaCO_3(aq) + H_2SO_4 \rightarrow Ca^{2+} + SO_4^{2-} + CO_2(g) + H_2O \quad (3)$$

Portlandite in contact with water drastically alters the pH of interaction at values higher than 12. However, carbonate alkalinity imparted by calcite dissolution in water involves the production of carbonic acid, whose dissociation yields pH slightly lower than that derived from portlandite dissolution ($9 < pH < 10$). This explains why the interaction of both AMDs with calcium mud (with portlandite) reaches pH values higher than the interaction with calcite

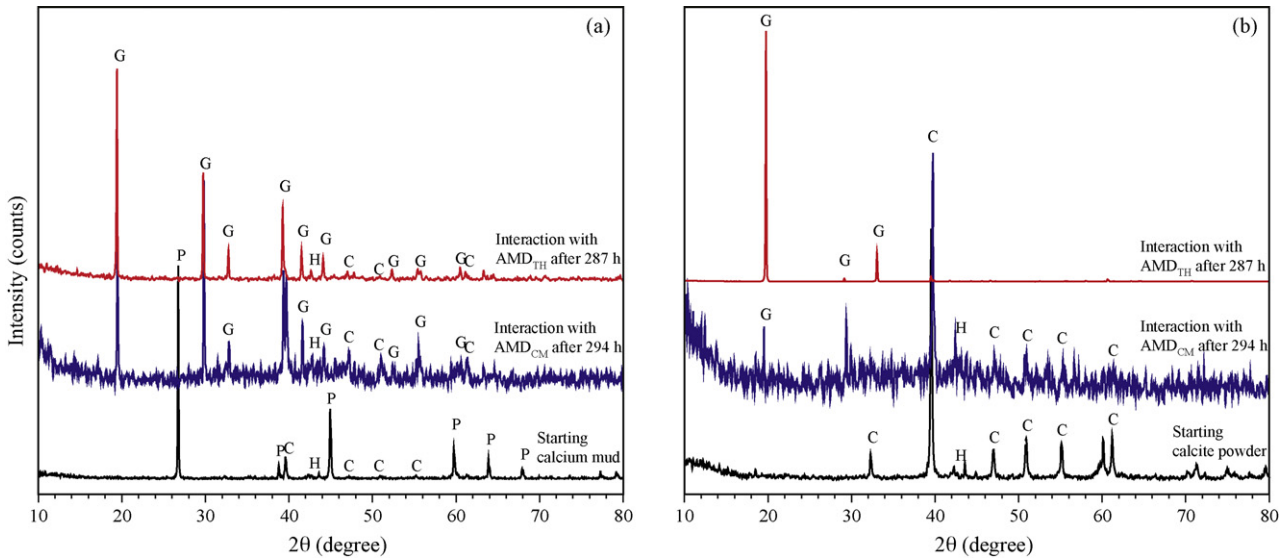

Fig. 4. XRD patterns of untreated (a) calcium mud and (b) calcite powder compared to final reaction products after the neutralization experiments. P: portlandite, C: calcite, H: hydroxyapatite, G: gypsum.

powder (without portlandite). Hydroxyapatite has demonstrated high metal removal efficiency by dissolution/precipitation, ion-exchange and specific sorption mechanisms [19,20]. Nevertheless, the role of hydroxyapatite as an alkaline additive is limited by its low solubility and neutralizing capacity (equilibrium pH around 4.5–5) in comparison with portlandite or calcite [21].

The presence of high concentrations of Ca from the alkaline additive dissolution and sulphate anions from AMD must favour the precipitation of gypsum in four interactions (Eq. (4)), which would explain the abundant existence of this mineral in the reaction products.

$$Ca^{2+} + SO_4^{2-} + 2H_2O \rightarrow CaSO_4{\cdot}2H_2O \quad (4)$$

On the other hand, the pH increase would cause the decrease in solubility of Fe and Al, and the subsequent precipitation by hydrolysis of amorphous or poorly crystallized oxy-hydroxides and/or oxy-hydroxysulphates. This process releases protons and buffer the pH at specific intervals (between 4.5 and 7) until both Fe and Al are

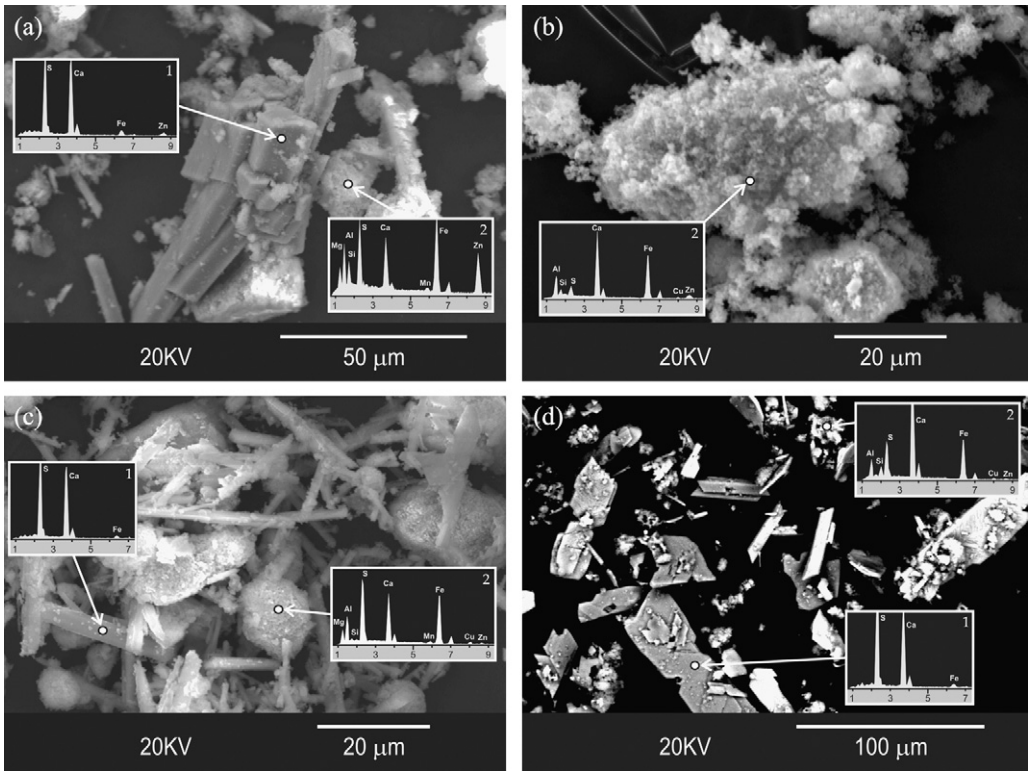

Fig. 5. SEM images of reaction products after the neutralization experiments (EDS spectra 1: gypsum crystals and 2: aggregates of newly formed amorphous phases): interactions (a) AMD$_{CM}$-CM, (b) AMD$_{CM}$-CP, (c) AMD$_{TH}$-CM and (d) AMD$_{TH}$-CP.

Table 2
Ideal reactions, equilibrium constants ($\log K_{eq}$) and saturation indices (SI) for supersaturated minerals resulting from the neutralization experiments. All equilibrium constants are from the database of model MINTEQ [16], except for schwertmannite.

Mineral	Reaction	$\log K_{eq}$	Saturation index			
			AMD_{CM}-CM	AMD_{CM}-CP	AMD_{TH}-CM	AMD_{TH}-CP
Starting minerals:						
Calcite	$CaCO_3 \Leftrightarrow Ca^{+2} + CO_3^{-2}$	−8.48	0.00	0.00	0.00	0.00
Hydroxyapatite	$Ca_5(PO_4)_3OH + H^+ \Leftrightarrow 5Ca^{+2} + 3PO_4^{-3} + H_2O$	−44.333	0.00	0.00	0.00	0.00
Portlandite	$Ca(OH)_2 + 2H^+ \Leftrightarrow Ca^{+2} + 2H_2O$	22.804	−8.96	–	−9.33	–
Newly formed sulphate and Fe–Al phases:						
$Al(OH)_3$(am)	$Al(OH)_3 + 3H^+ \Leftrightarrow Al^{+3} + 3H_2O$	10.8	1.17	2.40	1.81	3.03
Alunite	$KAl_3(SO_4)_2(OH)_6 + 6H^+ \Leftrightarrow K^+ + 3Al^{+3} + 2SO_4^{-2} + 6H_2O$	−1.4	4.26	11.85	3.93	13.19
Basaluminite	$Al_4(OH)_{10}SO_4 + 10H^+ \Leftrightarrow 4Al^{+3} + SO_4^{-2} + 10H_2O$	22.7	6.67	14.20	9.77	18.38
Boehmite	$AlOOH + 3H^+ \Leftrightarrow Al^{+3} + 2H_2O$	8.578	3.39	4.62	4.04	5.26
Diaspore	$AlOOH + 3H^+ \Leftrightarrow Al^{+3} + 2H_2O$	6.873	5.09	6.32	5.74	6.96
Ferrihydrite	$Fe(OH)_3 + 3H^+ \Leftrightarrow Fe^{+3} + 3H_2O$	4.891	6.87	5.93	7.45	4.56
Gibbsite	$Al(OH)_3 + 3H^+ \Leftrightarrow Al^{+3} + 3H_2O$	8.291	3.67	4.90	4.32	5.54
Goethite	$FeOOH + 3H^+ \Leftrightarrow Fe^{+3} + 2H_2O$	0.5	9.57	8.63	10.15	7.26
Gypsum	$CaSO_4{\cdot}2H_2O \Leftrightarrow Ca^{+2} + SO_4^{-2} + 2H_2O$	−4.848	0.24	0.23	0.92	0.81
Jarosite-K	$KFe_3(SO_4)_2(OH)_6 + 6H^+ \Leftrightarrow K^+ + 3Fe^{+3} + 2SO_4^{-2} + 6H_2O$	−14.8	11.95	13.01	11.43	8.35
Schwertmannite [a]	$Fe_8O_8(OH)_{8-2x}(SO_4)_x + (24-2x)H^+ \Leftrightarrow 8Fe^{+3} + xSO_4^{-2} + (16-2x)H_2O$	18 ± 2.5 [b]	26.01–31.01	23.25–28.25	31.63–36.63	15.34–20.34
Schwertmannite [a]	$Fe_8O_8(OH)_{8-2x}(SO_4)_x + (24-2x)H^+ \Leftrightarrow 8Fe^{+3} + xSO_4^{-2} + (16-2x)H_2O$	10 ± 2.5 [c]	33.51–38.51	30.75–35.75	39.13–44.13	22.84–27.84
Other newly formed metallic phases:						
$Cd(OH)_2$(am)	$Cd(OH)_2 + 2H^+ \Leftrightarrow Cd^{+2} + 2H_2O$	13.73	−3.57	−6.16	−4.31	−8.07
$Cr(OH)_3$(am)	$Cr(OH)_3 + H^+ \Leftrightarrow Cr(OH)_2^+ + H_2O$	−0.75	1.42	0.11	2.89	0.37
$Cu(OH)_2$	$Cu(OH)_2 + 2H^+ \Leftrightarrow Cu^{+2} + 2H_2O$	8.674	1.88	−0.11	2.40	−0.30
$Ni(OH)_2$	$Ni(OH)_2 + 2H^+ \Leftrightarrow Ni^{+2} + 2H_2O$	12.794	−1.97	−4.56	−1.99	−5.74
$Zn(OH)_2$(am)	$Zn(OH)_2 + 2H^+ \Leftrightarrow Zn^{+2} + 2H_2O$	12.474	0.90	−1.67	0.23	−3.52

[a] $x = 1.84$ according to Acero et al. [22].
[b] Thermodynamic data from Bigham et al. [23].
[c] Thermodynamic data from Yu et al. [24].

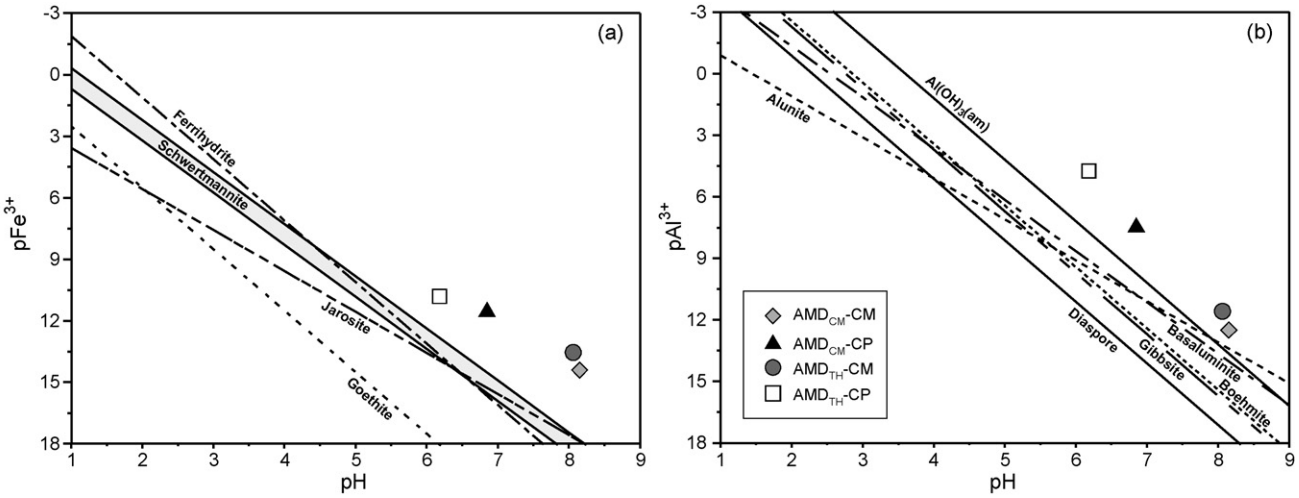

Fig. 6. Representation of (a) $\log(a_{Fe^{3+}})$ and (b) $\log(a_{Al^{3+}})$ vs. pH after the neutralization experiments (lines represent equilibrium of minerals according to ideal reactions and equilibrium constants shown in Table 2).

removed from the solution. Indeed, this is precisely the case of experiments where Fe and Al concentrations were below the detection limit and pH at the steady state was controlled by alkalinity of the starting materials.

PHREEQC calculations predicted supersaturation in the aforementioned phases. Several thermodynamic simulations were performed considering acid water in contact with the starting alkaline additives according to ratios described in Section 3.2. End of computer interactions showed a state of equilibrium for calcite and hydroxyapatite (SI = 0) in all experiments, and subsaturation (SI < 0) for portlandite in the case of experiments with calcium mud (Table 2). Neutralization process by dissolution of starting minerals occurs until equilibrium with the solutions is reached. Achievement of equilibrium depends on initial amount of acidity neutralizing minerals. In the case of calcite and hydroxyapatite, and according to PHREEQC, there are enough amounts to achieve equilibrium, at which time would cease to be dissolved and an unreacted excess would not intervene in the neutralization. However, in experiments with calcium mud, portlandite amount is not enough to reach equilibrium and this mineral is completely dissolved, as it is shown by negative SI value.

After reaction, the modelling code indicates that the solutions are supersaturated for all interactions with respect to gypsum and oxy-hydroxides and/or oxy-hydroxysulphates of Fe–Al (Table 2). The Fe phases which control Fe solubility in the neutralization experiments are minerals of the jarosite group, schwertmannite, ferrihydrite and goethite. On the other hand, Al solubility seems to be controlled by a mixture of phases like amorphous $Al(OH)_3$, alunite, basaluminite, boehmite, diaspore and gibbsite. Applying the law of mass action to dissolution ideal reactions of oxy-hydroxides and/or oxy-hydroxysulphates of Fe–Al and considering their $\log K_{eq}$ (Table 2), and assuming that a_{H_2O} equals 1, one can calculate and plot the equilibrium lines as a function of $pFe^{3+} = -\log(a_{Fe^{3+}})$ and $pAl^{3+} = -\log(a_{Al^{3+}})$ vs. pH (supersaturation above equilibrium and subsaturation below equilibrium; Fig. 6). The values obtained in PHREEQC simulations for all interactions suggest the supersaturation of leachates with respect to these minerals. Although solutions are theoretically supersaturated in these Fe oxy-hydroxides and/or oxy-hydroxysulphates, ferrihydrite appears to be the most stable phase thermodynamically, as shown in the sulphur–iron pε–pH stability diagram (Fig. 7).

PHREEQC calculations are totally consistent with the mineralogical characterization of final solid products. As for the starting minerals, an unreacted excess of calcite and hydroxyapatite was identified by XRD at the end of the experiments with both alkaline additives, while portlandite diffraction pattern is absent in XRD diagram of the reaction products of the experiments with calcium mud which supports the assertion of its complete dissolution. On the other hand, and as for the newly formed phases, gypsum was recognized by both XRD and SEM-EDS, while amorphous Fe–Al oxy-hydroxides and/or oxy-hydroxysulphates only by

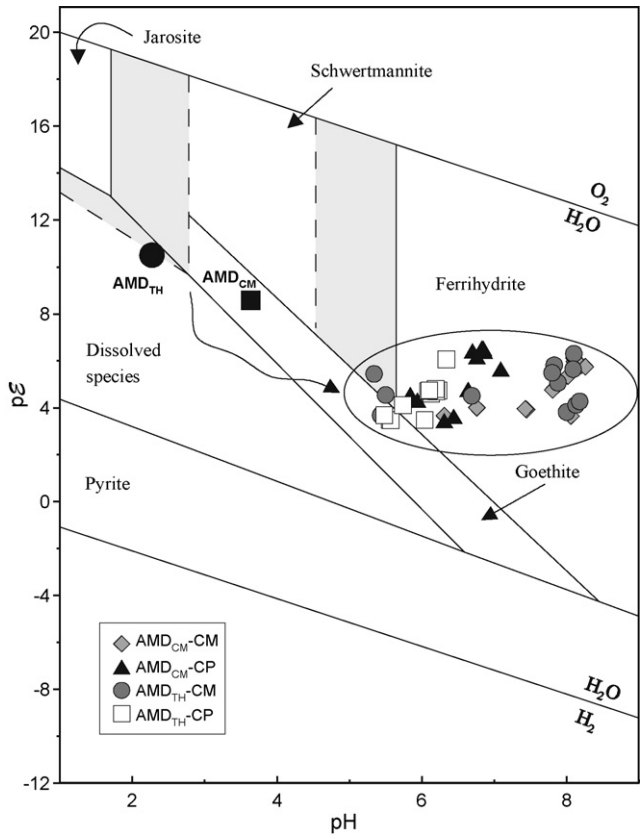

Fig. 7. Eh and pH projection into a sulphur–iron pε–pH diagram for the solutions resulting from the neutralization experiments. The pε–pH diagram is for the system Fe–S–K–O–H at 25 °C and 1 bar pressure; assuming pe = Eh(mv)/59.2 and total log activities of $Fe^{2+} = -3.47$; $Fe^{3+} = -3.36$ or -2.27; $SO_4^{-2} = -2.32$, $K^+ = -3.78$. Darker areas show possible expansion of K-jarosite and ferrihydrite fields. Modified from Bigham et al. [23].

SEM-EDS (undetectable by XRD) as micrometric agglomerates of globular phases chemically composed mainly of S, Fe and Al.

Precipitation of mainly gypsum, and at a less extent of metal oxy-hydroxysulphates, results in the decrease of sulphate concentration with an average removal rate of 40 and 72% at the end of the experiments with AMD_{CM} and AMD_{TH}, respectively. Whereas precipitation of Fe–Al oxy-hydroxides and/or oxy-hydroxysulphates cleans up both AMDs and justifies the below detection limits concentrations of Fe and Al recorded in solutions resulting from all interaction experiments.

It has long been known that the minimum solubility of hydroxides of trivalent metals such as Fe, Al and Cr is at pH between 6 and 8, however, the solubility of hydroxides of divalent metal such as Cd, Cu, Ni and Zn begins to decrease at pH > 8 [25]. The pH reached by starting material dissolution favours the supersaturation of the solutions with respect to amorphous hydroxides of trivalent metals such as Cr, in addition to Fe and Al as discussed above. Albeit, the high pH values needed to supersaturate the solutions with respect to hydroxides of divalent metals such as Cu and Zn and remove them from acid water seem to be reached only by means of calcium mud owning to portlandite dissolution. None of the interactions achieves the pH needed for minimum solubility of Cd and Ni, and solutions are not supersaturated in their respective hydroxides (Table 2). Nevertheless, another effective mechanism in removing trace metals dissolved in AMD solution involves the co-precipitation and/or adsorption onto amorphous Fe–Al oxy-hydroxides and/or oxy-hydroxysulphates, as previously reported in numerous investigations [23,26,27]. In fact, some trace metals were identified in the EDS analytical results together S, Fe and Al in the aggregates of newly formed amorphous phases.

The removal rates at the steady state of metals by precipitation, co-precipitation and adsorption as metallic oxy-hydroxides and/or oxy-hydroxysulphates with respect to initial AMD were total (approx. 100%) in the interactions of calcium mud with both acidic waters in the most of elements analyzed, i.e., Fe, Al, Zn, Cu, Cd, Ni, As and Cr. In the experiments with calcite powder, the average removal rates of Fe, Al, As, Cu and Cr were also of about 100%; however, the retention process was partial for Cd (≈80%), Zn (≈56%) and Ni (≈33%). It seems to be that removal rates of Ni and Cd in experiments with calcium mud, and Cu, Cd, Ni and Zn in the experiments with calcite powder is exclusively attributable to processes of co-precipitation and/or adsorption onto amorphous Fe–Al oxy-hydroxides and/or oxy-hydroxysulphates, since the final pH is not sufficient to achieve the minimum solubility of their hydroxides. This process alone is so effective in metal retention that explains a decrease of Zn concentrations in solution of up to 135 and 250 mg L^{-1} in the interactions between calcite powder and AMD_{CM} and AMD_{TH}, respectively. The formation of the newly formed amorphous phases also promoted the removal of the additional toxic elements contained in both alkaline additives and that surely were released into solution when dissolved. Therefore, utilization of calcium mud and calcite powder would not contribute to contamination with additional metals other than those already existing in AMD.

5. Possible environmental and economic benefits

Calcium mud from cellulose pulp production offers a hopeful solution for the passive treatment of AMD. The application of this waste inevitably requires establishing a balance between the exact amount to be used and the greatest possible economic and environmental benefits. This balance involves achieving the best possible quality of the resulting solutions during the neutralization, avoiding an excess of unreacted alkaline additive after treatment, and so avail the best possible annual produced amount without losing anything. Moreover, an excess of alkaline additive, concretely portlandite, would raise pH up to 12, value from which would increase again the solubility of metal hydroxides (e.g. Al) and make inappropriate the passive treatment.

Treatment optimization can be performed using the PHREEQC computer tool by simulating interactions between variable amounts of alkaline additive and AMD. Results of these interactions are shown in Fig. 8. In the case of calcium mud, the optimum amount meeting all the treatment requirements is 0.05 and 0.35 g in 40 mL of AMD_{CM} and AMD_{TH}, respectively (Fig. 8a and c). These ratios would raise pH to approx. 6.5, would cause the total retention of Fe and Al by precipitation of oxy-hydroxides and oxy-hydroxysulphates, and all additive (both portlandite and calcite) would be completely consumed. The already proven process of adsorption and co-precipitation would cause the retention of remaining metals in solution. ENCE group generates annually 4500 t of calcium mud (and up to 65,000 t along with other

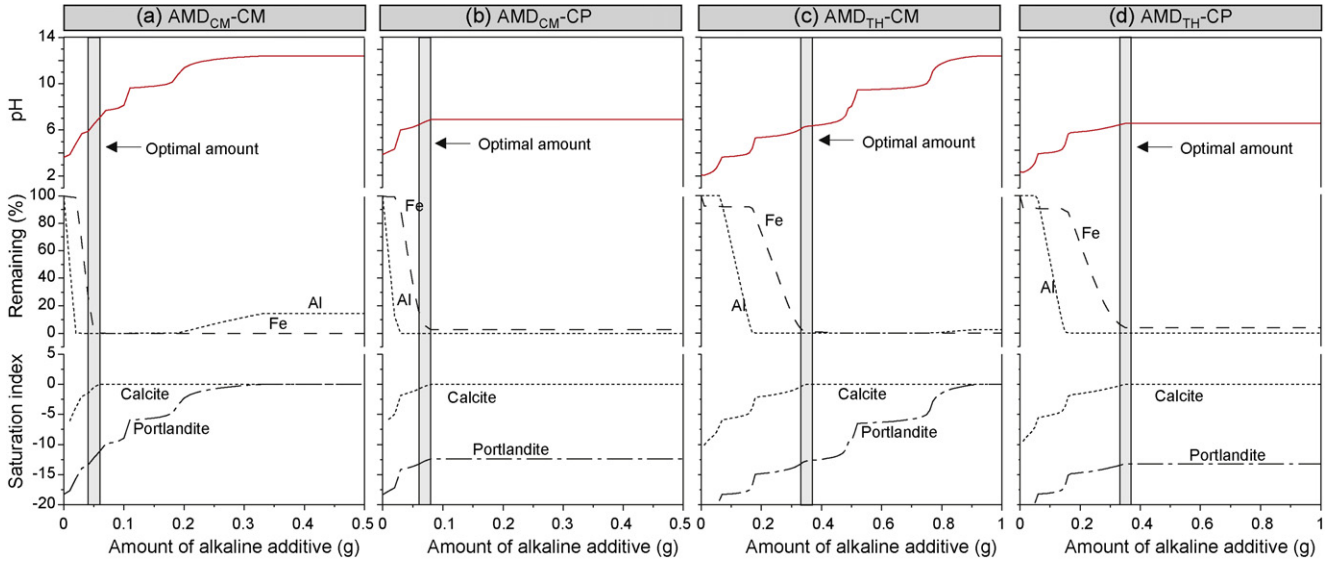

Fig. 8. Representation of (i) pH, (ii) Fe and Al remaining in solution and (iii) saturation indices of calcite and portlandite vs. amount of alkaline additive. Simulation performed with PHREEQC for the four interactions (a) AMD_{CM}-CM, (b) AMD_{CM}-CP, (c) AMD_{TH}-CM and (d) AMD_{TH}-CP. Vertical lines represent optimal treatment conditions (see explanation in text).

alkaline paper mill wastes) as a result of the production of 300,000–400,000 t of chlorine-free pulp on each of three cellulose pulp factories existing in Spain (Huelva, Pontevedra and Navia). With the experimental solid:liquid ratios, the annually produced calcium mud could effectively treat up to 1.8×10^9 and 3.6×10^8 L of AMD_{CM} and AMD_{TH}, respectively. However, extrapolating the optimal neutralizing capacity obtained in this study, the treatable volumes amount to 3.6×10^9 and 5.1×10^8 L, i.e. an average discharge of 114 and 16 L s^{-1}, of AMD_{CM} and AMD_{TH}, respectively.

In addition to neutralize AMD, Pérez-López et al. [12] previously reported an experimental system to sequester CO_2 using calcium mud, as stated before. The extrapolation of such experiments to a real industrial scale would suppose a CO_2 sequestration capacity of 220 kg of CO_2/t of calcium mud into 500 kg of stable calcite. If the total annual amount of calcium mud produced by ENCE-Spain, i.e. 4500 t, were targeted to reduce CO_2 emissions into the atmosphere, the mass balance of the process would result in the capture of 1000 t of CO_2 and the production of around 2200 t of calcite-rich waste. ENCE could sell CO_2 allowances worth €25,000/year (and up to €375,000 together with other alkaline wastes), avoiding other companies that do not obey with their emission rights to pay fines of up to €100,000/year (and up to €1,500,000 using other alkaline wastes). Purchase/sale of CO_2 allowances from emissions trading schemes within the Kyoto Protocol is described in detail elsewhere [12]. Recycling of 2200 t of calcite powder also would bring economic benefits to ENCE-Spain; in fact, in today's market that amount of natural calcite can cost around €200,000 (€0.08–0.12 per kg). Note that the price of calcite powder should be a little lower due to its content in toxic elements that can be released in solution when dissolves. These metals seem not to be a problem if calcite powder is applied for treating acidic waters, a successful application according to this study. Based on PHREEQC calculations, the optimal amount of calcite powder for reaching a pH of 6.2, total retention of Fe and Al, and complete dissolution of alkaline additive is 0.07 and 0.35 g in 40 mL of AMD_{CM} and AMD_{TH}, respectively (Fig. 8b and d). With the experimental ratios, 2200 t of calcite powder could neutralize satisfactory 8.8×10^8 L of AMD_{CM} and 1.8×10^8 L of AMD_{TH}. However, the treatment volumes with optimal ratios may reach up to 1.3×10^9 L of AMD_{CM} and 2.5×10^8 L of AMD_{TH}, i.e. an average annual discharge of 40 and 8 L s^{-1}, respectively.

Given that AMD_{CM} meets hydrogeochemical facies that are adjusted to average of typical acidic wastewaters from the IPB, results obtained in these interactions could be extrapolated to most discharges from the area. Discharge values of potentially treatable AMD_{CM} using calcium mud and calcite powder are 114 and 40 L s^{-1}, respectively. Albeit, the average discharge of AMD in the IPB is around 9 L s^{-1} [13]. Consequently, the annual production of both wastes could ensure treatment of at least the main sources of pollution of Tinto and Odiel rivers, and thus, reduce the pollution load reaching the Atlantic Ocean.

6. Conclusions

In search of the most effective alkaline additive for treatment of acid mine drainage (AMD) generated by sulphide oxidation in the Iberian Pyrite Belt (IPB), the calcium mud wasted from the production of pulp for paper manufacture by ENCE-Spain company fulfils all necessary expectations for the following reasons:

1. *High acid neutralizing potential*: The strongly alkaline nature of calcium mud (55 wt% portlandite and 33 wt% calcite) favours the efficient neutralization of the acidic waters in interaction. As shown by XRD and SEM-EDS techniques, and thermodynamic calculations with PHREEQC, the quality improvement of AMD is promoted by precipitation of gypsum along with a mixture of amorphous or poorly crystalline Fe–Al oxy-hydroxides and oxy-hydroxysulphates, which play a significant role in removing other metals from solution. In fact, final solutions reached the pre-potability requirements of water for human consumption under EU regulations.
2. *Low-cost*: Calcium mud is usually a stockpiled waste with low applicability due to its high metal concentrations. Hence, compared with typical alkaline additive (e.g., limestone), the main advantages of using calcium mud for neutralizing AMD could be its lower price. Moreover, the metals contained in this low-cost waste are also retained during AMD neutralization processes, and thus, would not mean an additional pollution source in the process.
3. *Production close to the demand*: Calcium mud production in Spain is around 4500 t. One of the main cellulose pulp plants in Spain is located at Huelva, relatively close to IPB (around 50 km), which further cheapens the transporting costs of this alkaline additive in a future treatment plan.
4. *Applicable to other environmental problems*: Some previous works have demonstrated that calcium mud could be also used to sequester CO_2 by aqueous carbonation and reduce greenhouse gas emissions into the atmosphere [12]. This process results in the production of a residual calcite powder that according to this study is also suitable for the AMD treatment. Mechanisms of acidity neutralization and metal retention using this calcite powder are similar to those observed with calcium mud. Considering the total annual of calcium mud, the calcite powder that would be produced by CO_2 sequestration could amount up to 2200 t.
5. *High treatment capacity*: According to our estimations, the amounts of calcium mud and calcite powder (potentially) produced per year could have capacity for the treatment of a common AMD with an average discharge of approx. 114 and 40 L s^{-1}, respectively. Taking into account average values of discharge for AMD from the IPB (ca. 9 L s^{-1}; [13]), both additives could be used for the remediation of the main acidic drainages of the region. Although calcite powder has a little less than half of capacity to treat AMD, its production would allow the double environmental application of calcium mud, i.e. first the reduction of CO_2 emissions into the atmosphere and subsequently the quality improvement of acidic discharges of the IPB.
6. *Economic benefits*: Obviously, using directly the calcium mud to neutralize AMD would impede its application to sequester carbon dioxide and some economic benefits concerning to selling of CO_2 emission rights and recycling of final calcite-rich products would be lost.

Definitely, the utilization of alkaline paper mill waste to treat AMD could mean the remediation of numerous sources of pollution in the IPB and the decrease of the pollutant load that is transported through the fluvial systems of the region to the Atlantic Ocean. This treatment is extensible to other areas historically contaminated by acidity and heavy metals where there is nearby cellulose pulp mill, a common industry worldwide.

Acknowledgements

This work has been financed by Spanish Ministry of Education and Science through project CTM2007-66724-C02/TECNO. The authors wish to express their gratitude to ENCE S.A. (San Juan del Puerto factory, Huelva) for samples of paper waste and the information offered. The analytical assistance of Rafael Carrasco, María José Ruiz, Gloria Blanco, María Paz Martín and others technicians from the Central Research Services of the University of Huelva is grate-

fully acknowledged. We thank Editor Dr. Joo Hwa Tay and three anonymous reviewers for their comments and helpful criticisms that significantly improved the quality of the manuscript.

References

[1] M. Kalin, A. Fyson, W.N. Wheeler, The chemistry of conventional and alternative treatment systems for the neutralization of acid mine drainage, Sci. Total Environ. 366 (2006) 395–408.
[2] PIRAMID Consortium, Engineering guidelines for the passive remediation of acidic and/or metalliferous mine drainage and similar wastewaters, in: European Commission Fifth Framework RTD Project No. EVK1-CT-1999-000021 "Passive In-situ Remediation of Acidic Mine/Industrial Drainage" (PIRAMID), University of Newcastle Upon Tyne, Newcastle Upon Tyne, UK, 2003.
[3] R.S. Hedin, G.R. Watzlaf, R.W. Nairn, Passive treatment of acid-mine drainage with limestone, J. Environ. Qual. 23 (1994) 1338–1345.
[4] C.R. Jage, C.E. Zipper, R. Noble, Factors affecting alkalinity generation by successive alkalinity-producing systems: regression analysis, J. Environ. Qual. 30 (2001) 1015–1022.
[5] T.S. Rötting, M.A. Caraballo, J.A. Serrano, C. Ayora, J. Carrera, Field application of calcite dispersed alkaline substrate (calcite-DAS) for passive treatment of acid mine drainage with high Al and metal concentrations, Appl. Geochem. 23 (2008) 1660–1674.
[6] P.L. Younger, A. Jayaweera, A. Elliot, R. Wood, P. Amos, A.J. Daugherty, A. Martin, L. Bowden, A.C. Aplin, D.B. Johnson, Passive treatment of acidic mine waters in subsurfaceflow systems: exploring RAPS and permeable reactive barriers, Land Contam. Reclam. 11 (2003) 127–135.
[7] R. Sáez, E. Pascual, M. Toscano, G.R. Almodóvar, The Iberian type of volcanosedimentary massive sulphide deposits, Miner. Deposita 34 (1999) 549–570.
[8] F. Nocete, E. Álex, J.M. Nieto, R. Sáez, M.R. Bayona, An archaeological approach to regional environmental pollution in the South-Western Iberian Peninsula related to Third Millennium BC mining and metallurgy, J. Archaeol. Sci. 32 (2005) 1566–1576.
[9] M. Olías, C.R. Cánovas, J.M. Nieto, A.M. Sarmiento, Evaluation of the dissolved contaminant load transported by the Tinto and Odiel rivers (South West Spain), Appl. Geochem. 21 (2006) 1733–1749.
[10] X. Querol, A. Alastuey, J.D. de la Rosa, A. Sánchez de la Campa, F. Plana, C.R. Ruiz, Source apportionment analysis of atmospheric particulates in an industrialised urban site in southwestern Spain, Atmos. Environ. 36 (2002) 3113–3125.
[11] A. Bellaloui, A. Chtaini, G. Ballivy, S. Narasiah, Laboratory investigation of the control of acid mine drainage using alkaline paper mill waste, Water Air Soil Pollut. 111 (1999) 57–73.
[12] R. Pérez-López, G. Montes-Hernández, J.M. Nieto, F. Renard, L. Charlet, Carbonation of alkaline paper mil waste to reduce CO_2 greenhouse gas emissions into the atmosphere, Appl. Geochem. 23 (2008) 2292–2300.
[13] J. Sánchez-España, E. López Pamo, E. Santofimia, O. Aduvire, J. Reyes, D. Barettino, Acid mine drainage in the Iberian Pyrite Belt (Odiel river watershed, Huelva, SW Spain): geochemistry, mineralogy and environmental implications, Appl. Geochem. 20 (2005) 1320–1356.
[14] G. Tyler, R. Carrasco, J.M. Nieto, R. Pérez-López, M.J. Ruiz, A.M. Sarmiento, Optimization of major and trace element determination in acid mine drainage samples by ultrasonic nebulizer-ICP-OES (USN-ICP-OES), in: Pittcon Conference, Chicago, USA, 2004, CD-ROM, Abst. # 9000-1000.
[15] D.L. Parkhurst, C.A.J. Appelo, PHREEQC-2 version 2. 12: A Hydrochemical Transport Model, 2005, http://wwwbrr.cr.usgs.gov.
[16] J.D. Allison, D.S. Brown, K.J. Novo-Gradac, MINTEQA2/PRODEFA2, A Geochemical Assessment Model for Environmental Systems. Version 3. 0 User's Manual, Environmental Research Laboratory, Office of Research and Development, US Environmental Protection Agency, EPA/600/3-911021, Athens, GA, 1991.
[17] A.M. Sarmiento, J.M. Nieto, M. Olías, C.R. Cánovas, Hydrochemical characteristics and seasonal influence on the pollution by acid mine drainage in the Odiel river Basin (SW Spain), Appl. Geochem. 24 (2009) 697–714.
[18] V. Ettler, O. Zelená, M. Mihaljevič, O. Šebek, L. Strnad, P. Coufal, P. Bezdička, Removal of trace elements from landfill leachate by calcite precipitation, J. Geochem. Explor. 88 (2006) 28–31.
[19] J.C. Choi, T.R. West, Y. Seol, Application of MINTEQA2 to the evaluation of apatite as a precipitant for acid mine drainage treatment, Environ. Eng. Geosci. 3 (1997) 217–223.
[20] I. Smičiklas, A. Onjia, S. Raičević, Đ. Janaćković, M. Mitrić, Factors influencing the removal of divalent cations by hydroxyapatite, J. Hazard. Mater. 152 (2008) 876–884.
[21] M.E. Hodson, E. Valsami-Jones, J.D. Cotter-Howells, Bonemeal additions as a remediation treatment for metal contaminated soil, Environ. Sci. Technol. 34 (2000) 3501–3507.
[22] P. Acero, C. Ayora, C. Torrentó, J.M. Nieto, The behavior of trace elements during schwertmannite precipitation and subsequent transformation into goethite and jarosite, Geochim. Cosmochim. Acta 70 (2006) 4130–4139.
[23] J.M. Bigham, U. Schwertmann, S.J. Traina, R.L. Winland, M. Wilf, Schwertmannite and the chemical modeling of iron in acid sulfate waters, Geochim. Cosmochim. Acta 60 (1996) 2111–2121.
[24] J.Y. Yu, B. Heo, I.K. Choi, J.P. Cho, H.W. Chang, Apparent solubilities of schwertmannite and ferrihydrite in natural stream waters polluted by mine drainage, Geochim. Cosmochim. Acta 63 (1999) 3407–3416.
[25] J.L. Cortina, I. Lagreca, J. De Pablo, J. Cama, C. Ayora, Passive in situ remediation of metal-polluted water with caustic magnesia: evidence from column experiments, Environ. Sci. Technol. 37 (2003) 1971–1977.
[26] M.M. Benjamin, J.O. Lecki, Multiple-site adsorption of Cd, Cu, Zn and Pb on amorphous iron oxyhydroxides, J. Colloid Interf. Sci. 79 (1981) 209–221.
[27] C.A. Cravotta, M.K. Trahan, Limestone drains to increase pH and remove dissolved metals from acidic mine drainage, Appl. Geochim. 14 (1999) 581–606.